

Early State Prediction Model for Offshore Jacket Platform Structural Using EfficientNet-B0 Neural Network

Le Anh-Hoang Ho^{1,2}, Viet-Dung Do¹, Xuan-Kien Dang^{1,*}, Thi Duyen-Anh Pham³

¹Artificial Intelligent in Transportation, Ho Chi Minh City University of Transport, Ho Chi Minh City 700000, Vietnam

²Faculty of Engineering and Technology, Van Hien University, Ho Chi Minh City 700000, Vietnam

³Institute of Languages & Social Sciences, Ho Chi Minh City University of Transport, Ho Chi Minh City 700000, Vietnam

Abstract

Offshore Jacket Platforms (OJPs) are often affected by environmental components that lead to damage, and the early detection system can help prevent serious failures, ensuring safe operations and mining conditions, and reducing maintenance costs. In this study, we proposed a prediction model based on Convolutional Neural Networks (CNNs) aimed at determining the early stage of the OJP structure's abnormal status. Additionally, the EfficientNet-B0 Deep Neural Network classifies normal and abnormal states, which may cause problems, by using displacement signal analysis at specific areas taken into account throughout the test. Displacement data is transferred to a 2D scalogram image by applying a continuous Wavelet converter that shows the state of the work. Finally, the scalogram image data set is used as the input of the neural network, and feasibility experimental results compared with other typical neural networks such as GoogLeNet and ResNet-50 have verified the effectiveness of the approach.

Received on 02 January 2024; accepted on 03 March 2024; published on 05 March 2024

Keywords: Identify damage, Offshore Jacket Platforms, Vibration-based assessment, Wavelet transformer, CNN, Confusion matrix

Copyright © 2024 L. A-H. Ho *et al.*, licensed to EAI. This is an open access article distributed under the terms of the [CC BY-NC-SA 4.0](#), which permits copying, redistributing, remixing, transformation, and building upon the material in any medium so long as the original work is properly cited.

doi:10.4108/eetinis.v11i2.4740

1. Introduction

Offshore Jacket Platforms (OJPs) are constantly subjected to environmental excitations such as sea waves, vessel acting, helicopter landing, and current wind loads. The dynamic reaction of the jacket platform under these loadings can be observed by installing devices such as accelerometer sensors. It should be noted that the weight of the top side of the OJP is significantly more than the weight of the other elements. Furthermore, the wave and vessel impact load pattern is remarkably close to the first mode shape of jacket constructions. The fact that structures are always subject to excitations is a distinguishing feature of the

maritime environment. Data processing and monitoring methods used to identify the abnormal status of offshore platforms must be capable of handling these kinds of excitations [1–4]. It is not possible to apply a conventional input-output framework since the input is frequently uncertain. Therefore, we need to find a solution to overcome this challenge.

Early detection of marine structural damage is necessary to avoid causing production disruptions and possible damage while reducing maintenance costs for the business in the long run. Therefore, the development of a structural status detection system to detect marine incidents promptly is an urgent task. To identify damage, a pyramidal structure is usually considered. The authors in [5] proposed an innovative damage typology approach. The damage states were divided into four levels: detection of the existence

*Corresponding author. Email: kien.dang@ut.edu.vn

of destruction, location, severity, and prediction of the harm. To determine the total deterioration of the system, information from the preceding level is required, and machine learning (ML) can be used as an effective algorithm. Therefore, algorithm based on Bayesian matrix learning is used for structural monitoring data imputation and response forecasting [6] to accomplish effective imputation and long-term structural response prediction. Furthermore, information is extracted from measurements using several conventional techniques that are based on mathematical principles; conversely, non-traditional approaches do not make any assumptions and rely on computational resources while using experimental principles. The simulated annealing technique [7] flexibility sensitivity-based approaches for evaluation in jacket-platform structures [8], and the artificial neural network (ANN) method [9–13] are both instances of these novel strategies. According to the analysis outcomes, mechanical technical experts may find this computationally advanced system beneficial in predicting the state of marine structures with a high degree of accuracy.

Vibration-based assessment is the most comprehensive way of predicting the structural health of offshore jet platforms (OJPs), and fluctuations in frequency were formerly considered indicators of degradation [14, 15]. As a result, a large number of studies have demonstrated that vibration is useful for determining the extent of structural damage, with frequencies changing essentially due to variations in mass and stiffness. On the topside of the OJP (Figure 1), accelerometers are naturally positioned to continuously monitor the vibration response to wave loadings. Actually, important requirements include ambient excitation to identify resonant frequencies, long-term vibration spectrum stability, the instruments' resilience in challenging conditions, and the ability to identify mode shapes from measurements performed above water level [16]. Unfortunately, this method only detects global faults, and it is unable to identify local fatigue cracks and tiny defects, which means that it frequently fails to reach the four standards mentioned in the text above. To solve these difficulties, modal forms are used as a frequency substitution and filtered using the Wavelet transformer due to their excessive sensitivity to Eigen frequencies.

Convolutional Neural Networks (CNNs) have been utilized more and more in recent years in order for the classification and detection of risks to construction structures by reducing the amount of input data based on the extraction of object properties [17–20]. However, during earthquakes and ocean waves, [17] employed a particular inertial damper to mitigate vibration on jacket offshore platforms. Furthermore, the method has been able to classify and predict the damage to the structure via the service of gathering neuron networks

in vibration-based harm assessment for construction structures [21–23]. The algorithm of a one-dimensional CNN automatically extracts damage-sensitive features from raw strain response data of a structure under specific excitation conditions without the need for manually generated feature extraction [24]. However, there have not been many experimental studies based on new CNN theories to increase prediction accuracy, especially not applying multiple-case testing to OJPs.

This paper represents an extension of the work described in [25]. In particular, we extend our previous work by using the EfficientNet-B0 neural network architecture to construct an early state prediction model (ESPM) to test the actual operation, showing how the performances of the proposed system compare. The results of this study are intended to support opportunities for both fixed and mobile offshore platforms to extend their lives, as well as to recommend localized maintenance strategies that minimize environmental and operational risk while saving energy output. Then, the main contributions of this work can be summarized as follows:

1. We collected the transmission signals on the fixed frame structure, and conducted experiments using the UT-OJP 02 model to collect displacement data sets from a sensor network. The raw data set can be represented as a data matrix.
2. We apply the continuous wavelet transform based on the data matrix and convert it to 2D scalogram images, which are used as inputs to train the EfficientNet-B0 network, which operates using a multi-target neural network structure to optimize accuracy.
3. Finally, we trained convolutional networks and tested, evaluation measures, which are quantitative metrics based confusion matrices that are used to evaluate the performance related to the accuracy of a proposed model.

The rest of the paper is organized as follows. The system model and the problem statement are provided in Section 2. Section 3 presents the method to collect data and images for the experimental process. The experiment and performance evaluation results are discussed in Section 4. Finally, Section 5 presents a discussion.

2. Problem statement

2.1. Offshore Jacket Platforms

The OJP has long been involved in offshore production activities, operating under harsh ocean conditions as the BK-9 OJP at Bach Ho oil field of Ba Ria - Vung Tau province, Southern Vietnam, as illustrated in Figure 1. In actual conditions, there are always arrangements for some components that force structural safety and reduce exploitation efficiency. Therefore, determining

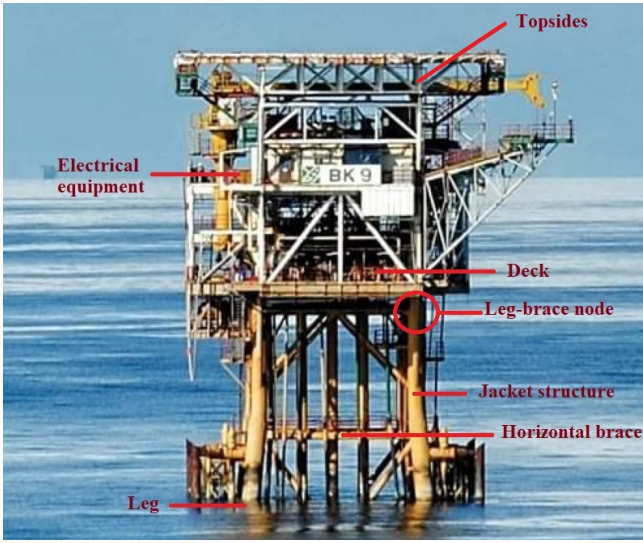


Figure 1. The OJP BK-9 at Ba Ria - Vung Tau Province, Vietnam.

environmental loads is an urgent task in the structural design process of offshore structures.

Table 1. Parameters of the OJP [26]

Parameter	Value
Water depth	25(m)
Jacket height	40.5(m)
Total number of floors	2
Total numbers of jacket legs	4
The pile diameter	1(m)
The wall thickness	0.02(m)
The weight of the upper deck	1600(ton)
The bottom size of the platform	11 x 11 (m ²)
The top area	6.75 x 6.75 (m ²)

The OJP is the seabed structure, which includes a topside module, jacket, and pile foundation. The jacket platforms not only have the ability to adapt well to environmental conditions but also achieve high safety and reliability. Therefore, these platforms become the main structural building for exploiting oil processing wells in shallow sea areas. Two different kinds of cross bracing (K and N types) are used in conjunction with V and X braces to establish the truss structure design. Working platforms, rig frames, and supporting equipment compose the structural model. Because of its two floors and multiple layers on top, the truss frame is especially remarkable. The horizontal braces of the deck truss structure are frame elements that firmly connect at the ends. The OJP is designed for shallow water depths of 25m. The structure has a legged jacket framework, with a pile diameter is 1m and a total height of 40.5m. Tables 1 [26] represent the Structural parameters of the actual OJP building

located at Liaodong Bay, Bohai Sea (China) with a similar structure to the Vietnamese BK-9 platform type as illustrated in Figure 1 [26].

2.2. Abnormal state of OJP structure

Evaluating the working status is challenging if the operator only uses a collection of displacement monitoring data, as this approach can sometimes lead to confusion. Data collected during OJP operations is saved to create an initial data set, then converted to a 2D scalogram for analysis to detect normal and abnormal OJP cases. In a normal state, the weather is encouraging for operations, and there is no influence on the OJP structure due to the anchoring of ships from outside. The scalogram image expressed by a large blue area with only a few yellow streaks visible, as shown in Figure 2(a).

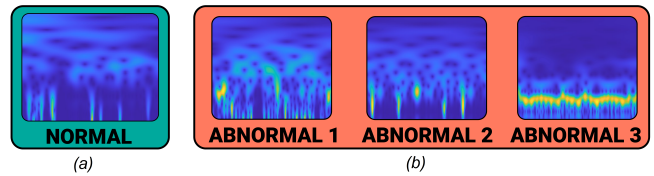


Figure 2. Transforming the OJP structure displacement to scalogram image.

In abnormal cases, strong waves at a certain frequency can impact the framework of machines operating on the OJP, which resonate with the structure’s magnetic fatigue effects, causing vibration on the surface. While the OJP is subjected to vibration causes damage to specific areas that have higher levels. The scalogram image displays yellow streaks interspersed with orange when there is an abnormality, as shown in Figure 2(b).

Remark 1: Environmental factors force the structure of the OJP to vibrate and evolve unbalanced. If the displacement level exceeds safe limitations, the building could collapse. Therefore, to ensure safety during operation, it is necessary to develop an ESPM to define the early stages of the harmful conditions. Additionally, it is important to note that monitoring the state of the structure is currently restricted to only a few local points, which leads to less accurate assessments.

3. Methodology

3.1. Data collection

The signal collection system is established on a designated structure that is designed with a steel frame in a 1 : 50 ratio to reality, as shown in Figure 3. The system has a height of 2.0195m and two stands measuring 70cm x 70cm each, the ESPM establishes a

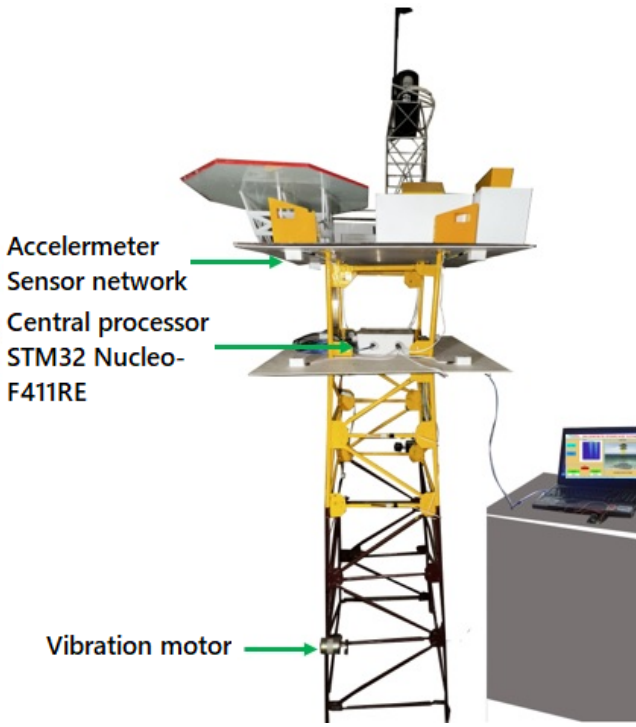


Figure 3. The overall diagram of the UT-OJP 02.

network of sensors at key locations throughout the structure. At these points, large displacements cause the structure to collapse. Moreover, the central processor receives a signal from eight sensors mounted on the stands, from which it sends data to the computer to predict the damage.

The UT-OJP 02 model uses an STM32 ARMCortex CPU, we determined the sampling rate should be set at 0.2 seconds based on the experimental results of the model. To be more precise, each of the 60 tests (K) involved 120 readings (I) from 8 monitoring sensor sites (J). 20 seconds on average were spent on each scalogram image. After that, apply the method to measure; this will take roughly 20 seconds. Thus, there is a 40-second variation between the total predicted time and the actual time. In this study, as illustrated in Figure 2, we offer four prediction states for the Offshore Jacket Platform so the offshore supervisor will comprehend to have a plan for rapidly fixing the damage states for OJP based on the level of damage. Moreover, it helps to prevent damage situations goes unnoticed or being discovered too late, resulting in accidents involving people and property loss. As a result, the raw data set from the sensor network can be represented as a matrix

$\mathbf{X}^{(k)} \in \mathcal{M}_{120,8}(\mathbb{R})$ as [27]

$$\mathbf{X}^{(k)} = \begin{pmatrix} x_{1,1}^{(k)} & x_{1,2}^{(k)} & \cdots & x_{1,8}^{(k)} \\ x_{2,1}^{(k)} & x_{2,2}^{(k)} & \cdots & x_{2,8}^{(k)} \\ \vdots & \vdots & \ddots & \vdots \\ x_{120,1}^{(k)} & x_{120,2}^{(k)} & \cdots & x_{120,8}^{(k)} \end{pmatrix} \quad (1)$$

In order to improve the efficiency of the training process, the input data sets are preprocessed by denoising [27]. Data scaling will improve the efficiency of neural network training for creating better prediction models. In this study, the data is scaled by column to fall within a specific range [0, 100]. Suppose that at k trials, we conduct the i -th sampling for each sensor location j . We get

$$M_j = \max(x_{ij}^{(k)}), i = 1, \dots, I, k = 1, \dots, K, \quad (2)$$

$$m_j = \min(x_{ij}^{(k)}), i = 1, \dots, I, k = 1, \dots, K, \quad (3)$$

where M_j and m_j represent the largest and smallest values of all the data in column j (with $j = 1, \dots, J$), respectively. As a result, the elements of the X matrix are scaled

$$y_{ij}^{(k)} := \left(x_{ij}^{(k)} - m_j \right) \frac{100}{M_j - m_j}, i = 1, \dots, I, j = 1, \dots, J, \quad (4)$$

$$k = 1, \dots, K$$

and Y matrix as

$$\mathbf{Y} = \begin{pmatrix} y_{1,1}^{(1)} & y_{1,2}^{(1)} & \cdots & y_{1,8}^{(1)} \\ \vdots & \vdots & \ddots & \vdots \\ y_{120,1}^{(1)} & y_{120,2}^{(1)} & \cdots & y_{120,8}^{(1)} \\ \hline y_{1,1}^{(2)} & y_{1,2}^{(2)} & \cdots & y_{1,8}^{(2)} \\ \vdots & \vdots & \ddots & \vdots \\ y_{120,1}^{(2)} & y_{120,2}^{(2)} & \cdots & y_{120,8}^{(2)} \\ \hline \vdots & \vdots & \ddots & \vdots \\ y_{1,1}^{(60)} & y_{1,2}^{(60)} & \cdots & y_{1,8}^{(60)} \\ \vdots & \vdots & \ddots & \vdots \\ y_{120,1}^{(60)} & y_{120,2}^{(60)} & \cdots & y_{120,8}^{(60)} \end{pmatrix} \quad (5)$$

We synthesize displacement data by operating vibration modules at four different vibration levels. These motors operate at varying frequencies to simulate both normal and abnormal states, such as huge waves or damage points. Each case involves capturing 120 scalogram images, with an average duration of 20 seconds per image. Finally, this process results in 800 measurements.

3.2. Scalogram image transform

The sensor network measures the displacement of the OJP model structure and transfers it to the STM central control unit. Displacement data is recorded for 8 sensor points during operation, resulting in a total of 800 measurements per spectrogram. This data is filtered by using the wavelet transformer and converted into a 224×224 pixel image [28, 29]. Environmental impacts have negative effects on the signals transmitted from sensors, which impact the EfficientNet-B0 neural network training process. To address this issue, the study applies the wavelet transformer [30] to remove noise from the data strings before converting them into a 2D scalogram image. As part of this study, the `wdenoise` function in Matlab's Wavelet toolbox is utilized to eliminate sensor measurement noise, with a quantization threshold of 3 [31]. These images are used as inputs to train the EfficientNet-B0 network.

The training data set for the CNN consists of 224×224 pixel RGB color images. These images are analyzed over time and represented on a 2D scalogram. The Continuous Wavelet Transformer (CWT) [32] is expressed in Equation 6, the wavelet function in time t is scaled and moved by parameters a and b , respectively, where the conversion interval and frequency are relative. Therefore, the scaled wavelet has the same energy as the parent wavelet, it always needs to be normalized by $1/\sqrt{a}$

$$W_{b,a}(t) = \frac{1}{\sqrt{a}} \psi\left(\frac{t-b}{a}\right) \quad (6)$$

The selected Wavelet function must effectively define the frequency properties of the signal to be modified. In this study, the Morlet (Gabor) Wavelet was used as a synthesis wavelet in the CWT function [32, 33]. The scalogram images will be employed as training data for the EfficientNet-B0 to learn the characteristics of the signal and to test the network.

3.3. Designing ESPM based on EfficientNet-B0 neural network

Google developed EfficientNet as a novel type of neural network that combines multiple layers to improve performance. This method systematically divides dimensions into depth, width, and resolution ratios. The ratio-sharing method used in EfficientNet balances these three components with a set of fixed ratio coefficients, resulting in better accuracy and efficiency compared to other cumulative networks [33]. Thus, the CNN is expanded in three dimensions: depth, width, and resolution. The depth of the CNN corresponds to the number of layers in the network [34–36]. The width is related to the number of neurons in each layer or the number of filters in each accumulated layer.

The resolution is simply the height and width of the input image. The data collected comprised 480 samples of wave distribution in both normal and abnormal states. These samples were subsequently filtered and transformed into 2D scalogram images. In Figure 4, we can see how an ESPM is designed using displacement data from a sensor network. The wavelet transformer converts these obtained results into images, which are used to construct an ESPM by the EfficientNet-B0 model. The predicted results indicate that the signal is effectively filtered by the wavelet transformer, and the images display unique features that can be applied for network training. To perform the training process, the image data set was split into two parts: 75% images for the training and 25% images for the testing.

Algorithm 1: Predicting the early state of the OJP model by using the ESPM algorithm

```

1 Initialization labeling the data set (scalogram images);
2 Initialization splitting the data set into train and test;
3 Initialization setting structural prediction model;
4 Configure the training parameters;
5 while  $epoch_m^{min} \leq epoch_m \leq epoch_m^{max}$  do
6   for each  $epoch\ m$  do
7     Set up Model on Matlab 2021 environment;
8     Train the EfficientNet-B0 model on Matlab;
9     Evaluate the ESPM with the loss
function (7) [34], and compare the latest profits
to the termination condition. If the convergence
condition is not met, increase  $m$  and go to Step 7.
10 end
11 end
12 Provide scalogram images for ESPM;
13 Predict the actual condition of the OJP model.
14 end

```

$$\mathcal{L} = \frac{1}{n} \sum_{i=1}^n (y_i - \hat{y}_i)^2 \quad (7)$$

Table 2. EfficientNet-B0 baseline network layers outline [33]

Stage	Operator	Resolution	Output Feature Maps	Layers
1	<i>Con3</i> × 3	224 × 224	32	1
2	<i>MBCConv1</i> , <i>k3</i> × 3	112 × 112	16	1
3	<i>MBCConv6</i> , <i>k3</i> × 3	112 × 112	24	2
4	<i>MBCConv6</i> , <i>k5</i> × 5	56 × 56	40	2
5	<i>MBCConv6</i> , <i>k3</i> × 3	28 × 28	80	3
6	<i>MBCConv6</i> , <i>k5</i> × 5	14 × 14	112	3
7	<i>MBCConv6</i> , <i>k5</i> × 5	14 × 15	192	4
8	<i>MBCConv6</i> , <i>k3</i> × 3	7 × 7	320	1
9	<i>Conv1</i> × 1 & <i>Pooling</i> & <i>FC</i>	7 × 7	1280	1

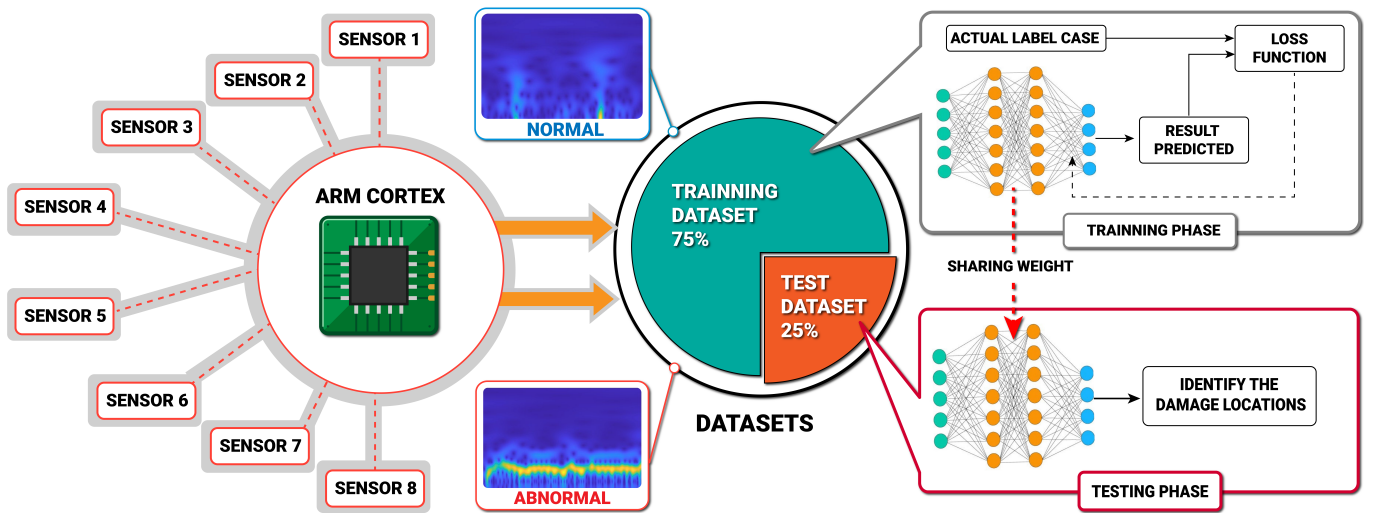


Figure 4. The schematic of the model for determining early state of OJP Structural.

Table 2 provides detailed information regarding the EfficientNet-B0 network structure, which includes 16 MBConv blocks varying in several aspects, for instance, kernel size, feature map expansion, and reduction ratio. Additionally, the authors propose the activation function as follows:

$$f(x) = x\sigma(x) \quad (8)$$

where $\sigma(x) = (1 + \exp(-x))^{-1}$ is the sigmoid function [36], and C is the total number of classes. The softmax activation function is defined [37]

$$s(y_i) = \frac{e^{y_i}}{\sum_{j=1}^C e^{y_j}} \quad (9)$$

This normalization limits the output sum to 1, so the softmax output $s(y_i)$ can be interpreted as the probability that the input belongs to the I class. y_i denotes the actual value from the testing data set, while \hat{y}_i presents the predicted value from the trained model. The complex ratio division method is intuitively demonstrated. If the input image is larger, the network needs more layers to enhance the reception and additional channels to get more detailed samples from the larger image [32]. The EfficientNet-B0 is a basic mobile-size network, which operates using a multi-target neural network structure to optimize accuracy. The design of the ESPM for predicting the condition of the OJP model is expressed in *Algorithm 1*.

4. Results and evaluation

4.1. Configuration parameter of the ESPM

The network training configuration parameters are as follows: miniBatchSize is 10, MaxEpochs is 30, and LearningRate is 0.0001. The results of EfficientNet-B0

network training are comparable to those represented in Figure 5. The training process carried 11 minutes and 19 seconds and resulted in an accuracy of 97.5%.

To verify the feasibility, the experimental result of EfficientNetB0 is compared to the GoogLeNet [38] and ResNet-50 [39], in the same experiment model. The parameters of the CNN models are defined in Table 3.

Table 3. Parameters of the CNN models

Elements	EfficientNet-B0	ResNet-50	GoogLeNet
Deep	82	50	22
Size	19.9 MB	96 MB	27 MB
Parameters	5.31 M	25.6 M	7 M
Input size	224 × 224 × 3	224 × 224 × 3	224 × 224 × 3

4.2. Evaluating the quality of CNN models

The new point of the algorithm in this study is that the authors first use Convolutional Neural Networks (CNN), specifically GoogLeNet, ResNet-50, and EfficientNet-B0, which are recent new algorithms to process input entered by images. Therefore, the collected data needs to be converted to spectral images to be able to distinguish the states and test results to achieve high accuracy. Compared to other NN structures, the CNN network has a less complex structure, especially testing on our model is 480 data sets for normal and abnormal cases, the time to train for OJP is not too long. Meanwhile, regarding the State Prediction Model for Offshore Jacket Platform Structural, there are not many studies on the same object, same parameters, and based on CNN as this method to compare effectiveness. In addition, evaluation is the measurement used to determine a prediction model's effectiveness. They are used in the

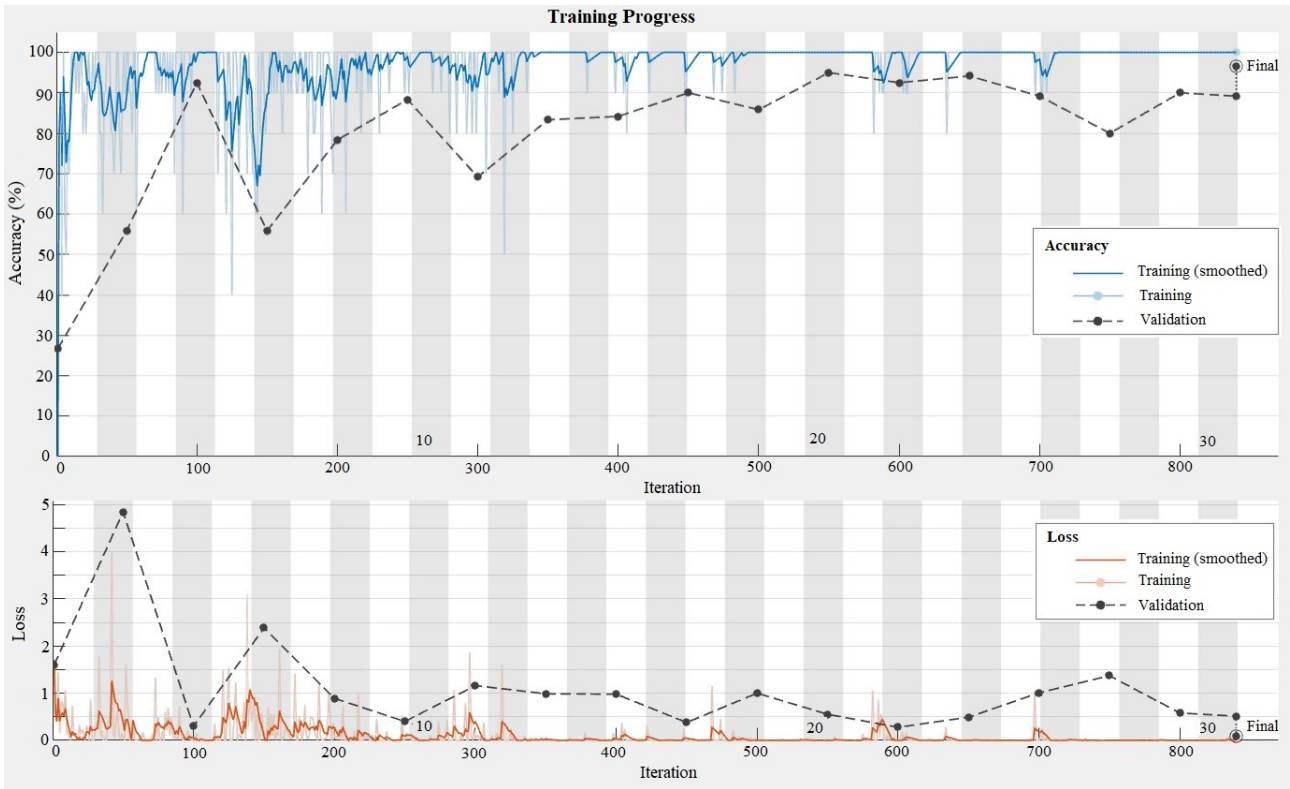


Figure 5. Results of training the EfficientNet-B0 network.

comparison of several models, the evaluation of how well they address a given issue, and the identification of areas in need of improvement. An accuracy and confusion matrix is used in this study’s evaluations. The number of true positive and true negative outcomes is divided by the total number of cases to get the accuracy of a diagnostic test or classifier. The variable TP refers to the number of correctly identified positive cases, while TN refers to the number of correctly identified negative cases. The accuracy is expressed by Equation 10 [40].

$$Accuracy = \frac{TP + TN}{TP + TN + FP + FN} \quad (10)$$

A confusion matrix is a summary of predicted results that measures various evaluation metrics, such as accuracy, recall, and precision. It provides an overview of the model’s performance by displaying the number of correct and incorrect predictions for each class. The compared CNN models are built under the same training conditions. The study tested the effectiveness of the EfficientNet-B0 network and compared it with other solutions using scalogram images from various data sets. The results are detailed in Table 4 and Figures 6 to 8.

The EfficiencyNet-B0 model takes longer to train than the GoogLeNet model, specifically 4 minutes and 24 seconds, due to the EfficiencyNet-B0’s deep feature extraction of the image sample set. Therefore, the

Table 4. Comparison results of the different CNN models

Model	Epochs	Learning rate	Training time (minute, second)	Accuracy (%)
GoogLeNet [38]	30	0.0001	6m and 55s	88.33
ResNet-50 [39]	30	0.0001	19m and 50s	93.5
EfficientNet-B0	30	0.0001	11m and 19s	97.5

ESPM is suitable for analyzing scalogram image sets and predicting the early state of the OJP model with complex structures. On the contrary, the accuracy of EfficientNet-B0 is better than the other two solutions, respectively 9.17% better than GoogLeNet and 4% better than ResNet-50. The ESPM ensures accurate prediction of OJP’s early states in actual operations, despite noise components, and meets Remark 1 requirements.

In addition, the evaluation of identification results with the EfficientNet-B0, GoogLeNet, and ResNet-50 network confusion matrix is shown in Figures 6 to 8. The results showed that EfficientNet-B0 takes less time to complete the training and achieves up to 97.5% accuracy. Meanwhile, the other two compared networks, GoogLeNet and ResNet-50, need more samples to learn with the same high accuracy. Because the EfficientNet-B0 can deeply extract characteristics

Output Class	Abnormal 1	Abnormal 2	Abnormal 3	Normal	
Abnormal 1	95 23.8%	5 1.2%	0 0.0%	0 0.0%	95.0% 5.0%
Abnormal 2	5 1.2%	95 23.8%	0 0.0%	0 0.0%	95.0% 5.0%
Abnormal 3	0 0.0%	0 0.0%	100 25.0%	0 0.0%	100% 0.0%
Normal	0 0.0%	0 0.0%	0 0.0%	100 25.0%	100% 0.0%
	95.0% 5.0%	95.0% 5.0%	100% 0.0%	100% 0.0%	97.5% 2.5%
	Abnormal 1	Abnormal 2	Abnormal 3	Normal	

Figure 6. Evaluate the recognition results with the error matrix of the EfficientNet-B0 network.

Output Class	Abnormal 1	Abnormal 2	Abnormal 3	Normal	
Abnormal 1	80 20.0%	0 0.0%	0 0.0%	16 4.0%	83.3% 16.7%
Abnormal 2	20 5.0%	100 25.0%	0 0.0%	8 2.0%	78.1% 21.9%
Abnormal 3	0 0.0%	0 0.0%	100 25.0%	0 0.0%	100% 0.0%
Normal	0 0.0%	0 0.0%	0 0.0%	76 19.0%	100% 0.0%
	80.0% 20.0%	100% 0.0%	100% 0.0%	76.0% 24.0%	89.0% 11.0%
	Abnormal 1	Abnormal 2	Abnormal 3	Normal	

Figure 7. Evaluate the recognition results with the error matrix of the GoogLeNet network.

of scalogram images in depth, it enables it to achieve high accuracy. Moreover, image samples are established from the data set of all sensor points, thereby providing overall early-state prediction results that overcomes the issues mentioned in Remark 1. The ESPM was tested on several different simulated damaged states with the impact generated by the vibration motor mounted on

Output Class	Abnormal 1	Abnormal 2	Abnormal 3	Normal	
Abnormal 1	100 25.0%	0 0.0%	0 0.0%	0 0.0%	100% 0.0%
Abnormal 2	0 0.0%	72 18.0%	0 0.0%	0 0.0%	100% 0.0%
Abnormal 3	0 0.0%	0 0.0%	100 25.0%	0 0.0%	100% 0.0%
Normal	0 0.0%	28 7.0%	0 0.0%	100 25.0%	78.1% 21.9%
	100% 0.0%	72.0% 28.0%	100% 0.0%	100% 0.0%	93.0% 7.0%
	Abnormal 1	Abnormal 2	Abnormal 3	Normal	

Figure 8. Evaluate the recognition results with the error matrix of the ResNet-50 network.

the model. Although the results are possible, the ESPM has only been tested in three cases of abnormalities with different displacement signals. The signal in the time domain, as well as the 2D scalogram image, showed the differences between test cases, so the results were received with high accuracy.

5. Conclusion

In this paper, we proposed a new ESPM to determine the early stages of non-invasive OJP structures by using the EfficientNet-B0 Deep Neural Network. Then, the CWT transforms the displacement data matrix into a 2D scalogram image that determines the immediate state of the platform. The experimental results showed significance in determining normal and abnormal status in the case of OJP is affected by simulated signal impacts, giving early predictive results a high accuracy ratio. Furthermore, based on the confusion matrix, we demonstrated the effectiveness of the proposed model achieved higher accuracy than the other solutions, and helped improve reliability in OJP operations. In conclusion, this work is necessary to enhance the quality of sensor signals and reduce network training time to achieve higher accuracy and to use more easily in many applications.

References

[1] MARIE BELLE GHSOUB. *Structural health monitoring of offshore jacket platforms*. Politecnico di Torino, 2018.
 [2] VAZIRIZADE, S.M., AZIZSOLTANI, H., AND HALDAR, A. (2022) Reliability estimation of jacket type offshore

- platforms against seismic and wave loadings applied in time domain. *Ships and Offshore Structures* 17(1): 143-152. doi: 10.1080/17445302.2020.1827632, URL <https://doi.org/10.1080/17445302.2020.1827632>.
- [3] TAHERI, A., TADAYON, B., AND ERSHADI, C. (2022) Risk Assessment of Fixed Offshore Jacket Platforms: A Persian Gulf Case Study. *International journal of Coastal, offshore & environmental engineering* 7(2): 24-30. doi: 10.22034/IJCOE.2022.155145, URL <https://doi.org/10.22034/IJCOE.2022.155145>.
- [4] VO, N.S., MASARACCHIA, A., NGUYEN, L.D., AND HUYNH, B.C. (2018) Natural Disaster and Environmental Monitoring System for Smart Cities: Design and Installation Insights. *EAI Endorsed Transactions on Industrial Networks and Intelligent Systems* 5(16), e5. doi: 10.4108/eai.29-11-2018.156001, URL <https://doi.org/10.4108/eai.29-11-2018.156001>.
- [5] MALEKLOO, A., OZER, E., ALHAMAYDEH, M., AND GIROLAMI, M. (2022) Machine learning and structural health monitoring overview with emerging technology and high-dimensional data source highlights. *Structural Health Monitoring* 21(4): 1906-1955. doi: 10.1177/14759217211036880, URL <https://doi.org/10.1177/14759217211036880>.
- [6] REN, P., CHEN, X., SUN, L., AND SUN, H. (2021) Incremental Bayesian matrix/tensor learning for structural monitoring data imputation and response forecasting. *Mechanical Systems and Signal Processing* 158: 107734. doi: 10.1016/j.ymsp.2021.107734, URL <https://doi.org/10.1016/j.ymsp.2021.107734>.
- [7] SUN, M., STASZEWSKI, W.J., AND SWAMY, R.N. (2010) Smart sensing technologies for structural health monitoring of civil engineering structures. *Advances in Civil Engineering* 2010: 1-13. doi: 10.1155/2010/724962, URL <https://doi.org/10.1155/2010/724962>.
- [8] LIU, K., LIU, Z., SHEN, W., AND LI, M. (2023) Flexibility sensitivity-based approaches for damage evaluation in jacket-platform structures. *Applied Ocean Research* 139: 103710. doi: 10.1016/j.apor.2023.103710, URL <https://doi.org/10.1016/j.apor.2023.103710>.
- [9] LUENGO, M.M., SHAFIEE, M., AND KOLIOS, A. (2019) Data management for structural integrity assessment of offshore wind turbine support structures: data cleansing and missing data imputation. *Ocean Engineering* 173: 867-883. doi: 10.1016/j.oceaneng.2019.01.003, URL <https://doi.org/10.1016/j.oceaneng.2019.01.003>.
- [10] OH, B.K., GLISIC, B., KIM, Y., AND PARK, H.S. (2020) Convolutional neural network-based data recovery method for structural health monitoring. *Structural Health Monitoring* 19(2): 147592171989757. doi: 10.1177/1475921719897571, URL <https://doi.org/10.1177/1475921719897571>.
- [11] FAN, G., LI, J., AND HAO, H. (2019) Lost data recovery for structural health monitoring based on convolutional neural networks. *Structural Control and Health Monitoring* 26(10): 1-21. doi: 10.1002/stc.2433, URL <https://doi.org/10.1002/stc.2433>.
- [12] LI, Y., BAO, T., CHEN, H., ZHANG, K., SHU, X., CHEN, Z., AND HU, Y. (2021) A large-scale sensor missing data imputation framework for dams using deep learning and transfer learning strategy. *Measurement* 178: 109377. doi: 10.1016/j.measurement.2021.109377, URL <https://doi.org/10.1016/j.measurement.2021.109377>.
- [13] FAN, G., LI, J., AND HAO, H. (2020) Vibration signal denoising for structural health monitoring by residual convolutional neural networks. *Measurement* 157: 107651. doi: 10.1016/j.measurement.2020.107651, URL <https://doi.org/10.1016/j.measurement.2020.107651>.
- [14] SPANOS, N.A., SAKELLARIOU, J.S., AND FASSOIS, S.D. (2020) Vibration-response-only statistical time series structural health monitoring methods: A comprehensive assessment via a scale jacket structure. *Structural Health Monitoring* 19(3): 736-750. doi: 10.1177/1475921719862487, URL <https://doi.org/10.1177/1475921719862487>.
- [15] HEARI, M.H., LOTFI, A., DOLATSHAHI, K.M., ANH GOLAFSHANI, A.A. (2017) Inverse vibration technique for structural health monitoring of offshore jacket platforms. *Applied Ocean Research* 62: 180-198. doi: 10.1016/j.apor.2016.11.010, URL <https://doi.org/10.1016/j.apor.2016.11.010>.
- [16] FARRAR, C., AND WORDEN, K. (2013) Structural health monitoring a machine learning perspective. doi: 10.1002/9781118443118, URL <https://doi.org/10.1002/9781118443118>. Publisher: John Wiley & Sons, LTD ISBN: 978-1-119-99433-6.
- [17] XU, T., LI, Y., AND LENG, D. (2023) Mitigating jacket offshore platform vibration under earthquake and ocean waves utilizing tuned inerter damper. *Bulletin of Earthquake Engineering* 21: 1627-1650. doi: 10.1007/s10518-022-01378-z, URL <https://doi.org/10.1007/s10518-022-01378-z>.
- [18] YE, X.W., JIN, T., AND YUN, C.B. (2019) A review on deep learning-based structural health monitoring of civil infrastructures. *Smart Structures and Systems* 24(5): 567-586. doi: 10.12989/sss.2019.24.5.567, URL <https://doi.org/10.12989/sss.2019.24.5.567>.
- [19] AVCI, O., ABDELJABER, O., KIRANYAC, S., HUSSEIN, M., GABBOUJ, M., AND INMAN, D.J. (2017) A review of vibration-based damage detection in civil structures: From traditional methods to Machine Learning and Deep Learning applications. *Mechanical Systems and Signal Processing* 147: 107077. doi: 10.1016/j.ymsp.2020.107077, URL <https://doi.org/10.1016/j.ymsp.2020.107077>.
- [20] DANG, X.K., TRUONG, H.N., NGUYEN, N.V., AND PHAM, T.D.A. (2020) Applying convolutional neural networks for limited-memory application. *TELKOMNIKA (Telecommunication Computing Electronics and Control)* 19(1): 244-251. doi: 10.12928/telkomnika.v19i1.16232, URL <https://doi.org/10.12928/telkomnika.v19i1.16232>.
- [21] DANG, X.K., HO, L.A.H., NGUYEN, X.P., AND MAI, B.L. (2022) Applying artificial intelligence for the application of bridges deterioration detection system. *TELKOMNIKA (Telecommunication Computing Electronics and Control)* 20(1): 149-157. doi: 10.12928/telkomnika.v20i1.20783, URL <https://doi.org/10.12928/telkomnika.v20i1.20783>.
- [22] DYER, A.S., ZAENGLE, D., NELSON, J.R., DURAN, R., WENZLICK, M., WINGO, P.C., BAUER, J.R., ROSE, K., AND ROMEO, L. (2022) Applied machine learning model comparison: Predicting offshore platform integrity with gradient boosting algorithms and neural networks. *Marine Structures* 83: 103152. doi: 10.1016/j.marstruc.2021.103152, URL <https://doi.org/10.1016/j.marstruc.2021.103152>.

- [23] ABDELJABER, O., AVCI, O., KIRANYAZ, M.S., BOASHASH, B., SODANO, H., AND INMAN, D.J. (2018) 1-D CNNs for structural damage detection: Verification on a structural health monitoring benchmark data. *Neurocomputing* 275: 1308-1317. doi: 10.1016/j.neucom.2017.09.069, URL <https://doi.org/10.1016/j.neucom.2017.09.069>.
- [24] BAO, X., FAN, T., SHI, C., AND YANG, G. (2021) One-dimensional convolutional neural network for damage detection of jacket-type offshore platforms. *Ocean Engineering* 219: 108293. doi: 10.1016/j.oceaneng.2020.108293, URL <https://doi.org/10.1016/j.oceaneng.2020.108293>.
- [25] NGUYEN, X.P., DANG, X.K., HO, L.A.H., LUU, H.M., AND NGUYEN, N.T. (2024) Design of a scalogram-based data acquisition and processing system for a multi-sensor network application for marine structures. *10th International Conference on Coastal and Ocean Engineering (ICCOE 2024)*, Accepted.
- [26] TIAN, X., WANG, Q., LIU, G., LIU, Y., XIE, Y., AND DENG, W. (2019) Topology optimization design for offshore platform jacket structure. *Applied Ocean Research* 84: 38-50. doi: 10.1016/j.apor.2019.01.003, URL <https://doi.org/10.1016/j.apor.2019.01.003>.
- [27] PURUNCAJAS, B., VIDAL, Y., AND TUTIVÉN, C. (2020) Vibration-response-only structural health monitoring for offshore wind turbine jacket foundations via convolutional neural networks. *Sensors* 20(12): 1–19. doi: 10.3390/s20123429, URL <https://doi.org/10.3390/s20123429>.
- [28] PAL, K.K., AND SUDEEP, K.S. (2017) Preprocessing for image classification by convolutional neural networks. In *2016 IEEE International Conference on Recent Trends in Electronics, Information and Communication Technology, RTEICT 2016 – Proceedings* 1778–1781. doi: 10.1109/RTEICT.2016.7808140, URL <https://doi.org/10.1109/RTEICT.2016.7808140>.
- [29] SZEGEDY, C., LIU, W., JIA, Y., Sermanet, P., REED, S., ANGUELOV, D., ERHAN, D., VANHOUCHE, V., AND RABINOVICH, A. (2015) Going deeper with convolutions. *Proceedings of the IEEE Conference on Computer Vision and Pattern Recognition* 1-9.
- [30] YIN, Y., HU, Y., AND LIU, P. (2021) The research on denoising using wavelet transform. *International Conference on Multimedia Technology*. doi: 10.1109/ICMT.2011.6002276, URL <https://doi.org/10.1109/ICMT.2011.6002276>.
- [31] SORNSSEN, I., SUPPITAKSAKUL, C., AND TOONKUM, P. (2022) Mother wavelet performance evaluation for noise removal in partial discharge signals. *ECTI Transactions on Electrical Engineering, electronics, and communications* 20(3): 450-459. doi: 10.37936/ecti-eec.2022203.247521, URL <https://doi.org/10.37936/ecti-eec.2022203.247521>.
- [32] MASHRUR, F.R., ISLAM, M.S., SAHA, D.K., ISLAM, S.M.R., AND MONI, M.A. (2021) SCNN: Scalogram-based convolutional neural network to detect obstructive sleep apnea using single-lead electrocardiogram signals. *Computers in Biology and Medicine* 134: 104532. doi: 10.1016/j.compbiomed.2021.104532, URL <https://doi.org/10.1016/j.compbiomed.2021.104532>.
- [33] TAN, M., AND LE, Q. (2019) EfficientNet: rethinking model scaling for convolutional neural networks. *Proceedings of the 36th International Conference on Machine Learning* 97: 6105-6114.
- [34] FAHIM, M., SHARMA, V., CAO, T.V., CANBERK, B., AND DUONG, T.Q. (2022) Machine Learning-Based Digital Twin for Predictive Modeling in Wind Turbines. *IEEE Access*, 10: 14184–14194. doi: 10.1109/ACCESS.2022.3147602, URL <https://doi.org/10.1109/ACCESS.2022.3147602>.
- [35] MASH, D.S., GHANI, A., SEE, C.H., KEATES, S., AND YU, H. (2022) Using deep neural networks to classify symbolic road markings for autonomous vehicles. *EAI Endorsed Transactions on Industrial Networks and Intelligent Systems* 9(31): e2. doi: 10.4108/eetinis.v9i31.985, URL <https://doi.org/10.4108/eetinis.v9i31.985>.
- [36] LE, T.M., TAT, B.T.N., AND NGO, V.M. (2022) Automated evaluation of Tuberculosis using Deep Neural Networks. *EAI Endorsed Transactions on Industrial Networks and Intelligent Systems* 9(30): e4. doi: 10.4108/eetinis.v8i30.478, URL <https://doi.org/10.4108/eetinis.v8i30.478>.
- [37] SWAIN, D., PANDYA, K., SANGHVI, J., AND MANCHALA, Y. (2023) An intelligent fashion object classification using CNN. *EAI Endorsed Transactions on Industrial Networks and Intelligent Systems* 10(4): e2. doi: 10.4108/eetinis.v10i4.4315, URL <https://doi.org/10.4108/eetinis.v10i4.4315>.
- [38] HAN, S., LI, B., LI, W., ZHANG, Y., AND LIU, P. (2024) Intelligent analysis of corrosion characteristics of steel pipe piles of offshore construction wharfs based on computer vision. *Heliyon* 10: e24142. doi: 10.1016/j.heliyon.2024.e24142, URL <https://doi.org/10.1016/j.heliyon.2024.e24142>.
- [39] GALLEGO, C.V., AND LAZAKIS, I. (2022) Development of a time series imaging approach for fault classification of marine systems. *Ocean Engineering* 263: 112297. doi: 10.1016/j.oceaneng.2022.112297, URL <https://doi.org/10.1016/j.oceaneng.2022.112297>.
- [40] MOUSAVI, Z., VARAHRAM, S., ETTEFAGH, M.M., SADEGHI, M.H., AND RAZAVI, S.N. (2020) Deep neural networks-based damage detection using vibration signals of finite element model and real intact state: An evaluation via a lab-scale offshore jacket structure. *Structural Health Monitoring* 10(1): 1-27. doi: 10.1177/1475921720932614, URL <https://doi.org/10.1177/1475921720932614>.